

Mechanism of the 1992 Nicaragua tsunami earthquake

Kenji Satake

Department of Geological Sciences, University of Michigan

Abstract. The 1992 Nicaragua earthquake generated larger tsunamis than expected from its surface wave magnitude (M_S 7.2) and is known as a 'tsunami earthquake'. Seismological studies showed that the duration was very long for its size, about 100 s. Other studies have shown that the seismic moment estimated from tsunamis is an order of magnitude larger than that from seismic waves, even after the long duration is accounted for. Numerical computations of tsunamis from various fault models are made to reconcile this discrepancy. Comparison of calculated waveforms with tide gauge records shows that the fault width is 40 km, much narrower than the aftershock area, and extends only into the upper 10 km of the ocean bottom. Slip amount on the fault is estimated to be 3 m from amplitude comparisons. The fault length is estimated to be 250 km, slightly longer than the aftershock area, from comparison of the tsunami height distribution. The rigidity around the shallow fault may be smaller than that of a standard underthrust fault, and the seismic moment is estimated as 3×10^{20} Nm, consistent with the seismic observations. A slow rupture on the shallow fault, presumably in the subducted sediments, is responsible to the unusually large tsunami excitation.

Introduction

The 2 September 1992 Nicaragua earthquake generated tsunamis that caused extensive damage on the Pacific coast of Nicaragua despite its moderate surface wave magnitude (M_S 7.2). Field surveys for seismic intensity and tsunami run-up height [Abe *et al.*, 1993; Baptista *et al.*, 1993; Satake *et al.*, 1993] showed that the intensity was very small (maximum III in Modified Mercalli scale) but the tsunami run-up height was as large as 9.9 m above mean sea level. The earthquake size inferred from the weak intensity is as small as $M=6$, while the large tsunamis correspond to those from an earthquake as large as $M=8$ [Abe *et al.*, 1993]. These discrepancies indicate that this earthquake was an unusual 'tsunami earthquake' [Kanamori, 1972].

Seismological analysis of the Nicaragua earthquake [Ide *et al.*, 1993; Kanamori and Kikuchi, 1993; Satake *et al.*, 1993] showed that the focal mechanism of this event was a shallow dipping (15°) thrust type with its strike parallel to the middle America trench (Figure 1). This event is associated with a subduction of the Cocos plate beneath the Caribbean plate. The duration of the rupture process is about 100 s, unusually long for its size. The seismic moment M_0 , corrected for the long duration, is estimated as 3.4×10^{20} Nm ($M_w=7.6-7.7$). Numerical modeling of tsunamis from this earthquake have been made by Imamura *et al.* [1993] and Titov and Synolakis [1993]. Both studies reproduced the observed tsunami heights from a source model with a seismic

moment about 3×10^{21} Nm, assuming a standard rigidity of 3.4×10^{10} N/m². This seismic moment is an order of magnitude larger than that estimated from seismic wave analysis.

The purpose of this paper is to reconcile the discrepancy in seismic moment estimates from seismic wave analysis and tsunami modeling, and to find the mechanism of the unusual tsunami excitation. The smaller surface wave magnitude (M_S 7.2) than the moment magnitude (M_w 7.6-7.7) is attributed to the slow rupture process [Pelayo and Wiens, 1992]; however, it cannot explain the order of magnitude difference in seismic moment estimates because the estimated moment from the seismological analysis already accounts for the long duration. We make numerical computations of tsunamis from a seismological source model, and compare them with the observed data, both tide gauge records and run-up heights, to find a source model consistent with both the seismological and tsunami data.

Tsunami Data and Computation

The tsunami run-up heights along the Nicaraguan coast were measured by field surveys soon after the earthquake and are reported elsewhere [Abe *et al.*, 1993; Baptista *et al.*, 1993; Satake *et al.*, 1993]. The tsunami was also recorded on tide gauges at Corinto and Puerto Sandino (see Figure 1 for location). Figure 2 shows these tide gauge records after the tidal components were removed. The Corinto tide gauge record shows an impulsive tsunami with its maximum at 61 min after the origin time. There is a small fall (about 10 cm) of sea level before the first rise. The trough-to-peak amplitude is 49 cm. The Puerto Sandino record also shows a sea level fall of about 10 cm, followed by a very abrupt sea level rise which made the gauge go off-scale at 65 min after the origin time. The trough-to-peak amplitude is at least 117 cm. Tadepalli and Synolakis [1994] called such a waveform, a small fall followed by a larger rise of water level, "leading depression N -wave".

We make numerical computations of tsunamis along the Nicaraguan coast using both linear shallow water equations and non-linear equations including bottom friction. The computational area with bathymetry is shown in Figure 1. The grid size is basically 1 min, but smaller (1/5 min) grids are used near the tide gauge stations in order to accurately represent local topography. The coastal depth on 1 min grid is about 10 m. The depth at the tide gauge station is 10 m in Corinto and 4 m in Puerto Sandino. The details of numerical computations, as well as comparison of linear and nonlinear computations, can be found in Satake [1994]. The vertical displacement field from faulting [e.g., Okada, 1985] is computed and used as initial conditions. Tsunami waveforms were output on coastal grid points as well as the tide gauge stations for comparison with the observed data.

Fault Width

We first make linear computation of tsunamis from a seismological fault model [Ide *et al.*, 1993]; the fault length along the strike, L , is 200 km, the down-dip width, W , is 100 km and

Copyright 1994 by the American Geophysical Union.

Paper number 94GL02338
0094-8534/94/94GL-02338\$03.00

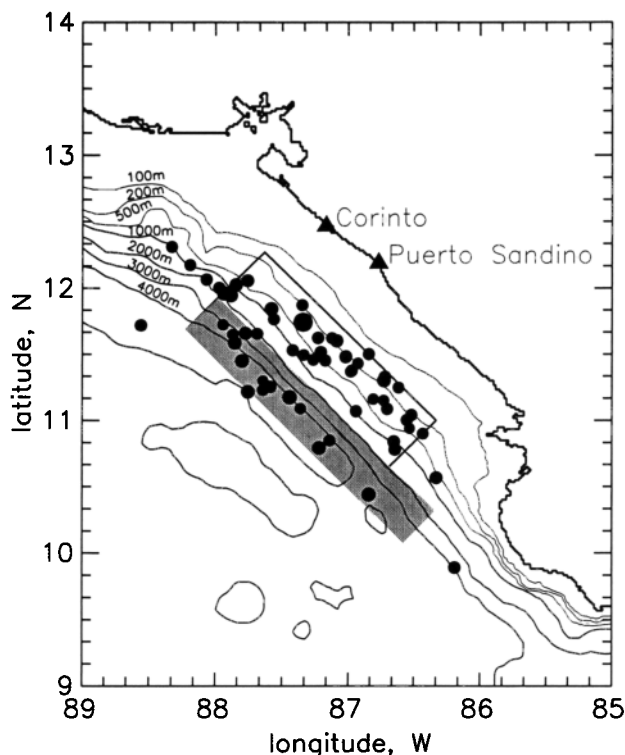


Figure 1. Map of the 1992 Nicaragua earthquake source region. Tsunami computations were made in this region using the shown bathymetry data. Solid circles show the aftershocks within 1 day of the mainshock (from Preliminary Determination of Epicenters). Open frame shows the seismological fault model [Ide *et al.*, 1993] whereas the shaded frame is the tsunami fault model of this study.

the average slip, u , is 0.5 m. Assuming a rigidity of 3×10^{10} N/m² for the top 25 km of the ocean bottom, these parameters give a seismic moment of 3×10^{20} Nm. Figure 2 shows a comparison of the observed (top) and the computed (bottom) waveforms. The computed tsunamis have much smaller amplitudes than the observed. In addition, the computed tsunamis from $W=100$ km model arrive too early and the period is too long compared to the observed at both stations.

Figure 3 shows a vertical deformation pattern along the cross-section of a subduction earthquake. The top edge of the fault is located at the trench axis. If the fault is 100 km wide, the vertical uplift extends toward land and the tsunami arrival becomes early. If the fault is narrower, say 40 km, the vertical deformation is limited in a smaller area and the tsunami would arrive at the coast later. The slip, and consequently the amount of vertical deformation, becomes larger for a narrower fault, if the seismic moment is constant, because it is given as $M_0 = \mu u L W$ where μ is the rigidity around the fault.

Based on the above qualitative examination, we carried out linear tsunami computations for different fault widths: 80 km, 60 km, 40 km and 20 km. The seismic moment is kept constant, so the slip amount is different for each width; for example, the slip is 1.25 m for the width of 40 km. The computed waveforms are also shown in Figure 2. The waveforms from narrower faults are similar to the observed. Judging from the shape (small fall of water level followed by a sharp rise), we conclude that the fault width is about 40 km, much narrower than 100 km. Since the fault dip is 15° and the top edge is located at the trench axis (the

ocean depth is about 5 km), the fault extends only 15 km below the sea level, or into the top 10 km of the crust. The surface projection of this narrow fault is shown as a shaded frame in Figure 1. It is much narrower than the 1-day aftershock distribution. This indicates that a small amount of slip might have occurred at deeper depth, but most of the coseismic slip is confined on the top 40 km down-dip section of the fault.

Fault Slip

In the linear tsunami calculation, the amplitude is proportional to slip amount on the fault. We compare the observed and calculated amplitudes from the $W=40$ km model at both stations. At Corinto, the amplitude ratio (obs/cal) is 5.4 for the first trough, 2.3 for the following peak. At Puerto Sandino, the ratio is 1.3 for the first trough; the following peak went off-scale. The geometric average of the three ratios is 2.5. By multiplying this to the assumed slip amount (1.25 m) for the $W=40$ km model, the fault slip u is now estimated to be 3 m.

The tsunami waveforms are computed again from these fault parameters using non-linear shallow water equation with bottom friction. As discussed in Satake [1994], inclusion of the non-linear terms does not significantly alter the initial part of the tsunami waveforms, although the maximum amplitudes usually become smaller because of the bottom friction terms. The comparison of tsunami waveforms are shown in Figure 4. The computed tsunami waveforms are very similar to the observed, although the amplitudes are slightly smaller.

Comparison with Run-up Heights

We now compare the maximum tsunami heights on coast calculated from the non-linear computation to the observed run-up heights. Since our computation does not include the run-up effect, we do not expect to match the amplitudes very well. In order to make numerical computations of tsunami run-ups [e.g., Shuto, 1991], the coastal topography as well as bathymetry must

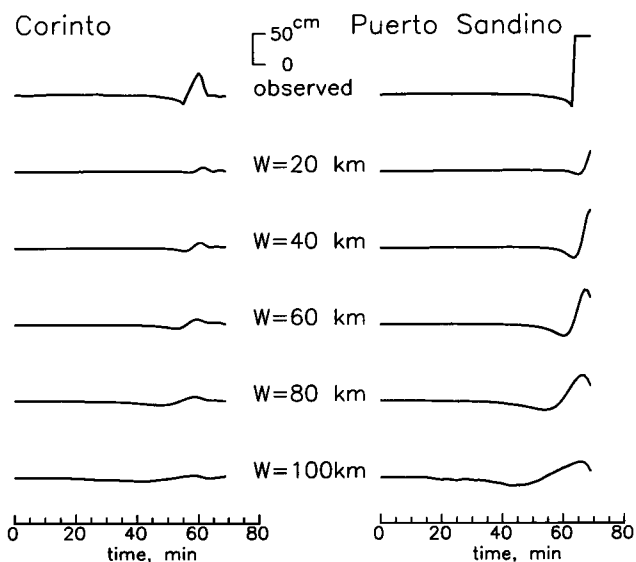


Figure 2. The observed tide gauge records (top) and the computed tsunami waveforms from models with different fault width. The time is measured from the origin time of the earthquake. See Figure 1 for the location of tide gauge stations.

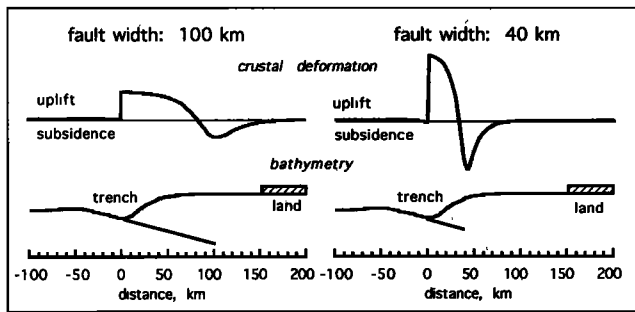


Figure 3. Schematic cross-section of fault for a subduction zone earthquake and the vertical deformation of ocean bottom.

be accurately known and a fine grid system must be used. Unfortunately, such data do not exist for the Nicaraguan coast. Here we will compare the general pattern of the tsunami height distribution. It is also interesting to find the amplification factor, a ratio between the run-up height to the tsunami amplitude in shallow water.

For computed tsunami heights, we use the maximum amplitude within 3 hours of the origin time. Figure 5 compares the maximum amplitudes along the coast (as a function of latitude) and the observed run-up heights above mean sea level (MSL). The tsunami arrived about an hour after the high tide when the sea level was about 50 to 80 cm above MSL, depending on the location and the actual arrival time of the maximum tsunamis. Even when we consider this correction, the observed run-up heights are much larger than the computed heights, about a factor of 3. In other words, the average amplification factor is 3.

The tsunami run-up heights were measured in the vicinity of tide gauge stations at Corinto and Puerto Sandino. At Corinto, the run-up height was 2.7 m above MSL, or about 2 m above the sea level at the tsunami arrival. This is about 5 times larger than the amplitude (40 cm) on the tide gauge record. At Puerto Sandino, the observed run-up height was 3.7 m above MSL or 2.9 m above the sea level at tsunami arrival. The tide gauge went off-scale but the amplitude was at least 1 m. Hence the amplification factor at this site is less than 3. The average factor, 3, estimated in our computation, lies between the two observed values.

There is no simple theoretical work to compare the predicted tsunami heights and the run-up heights. *Imamura et al.* [1993] assumed that the factor is 2, based on experimental data on beach with a slope of 1/10. *Titov and Synolakis* [1993] combined a two-

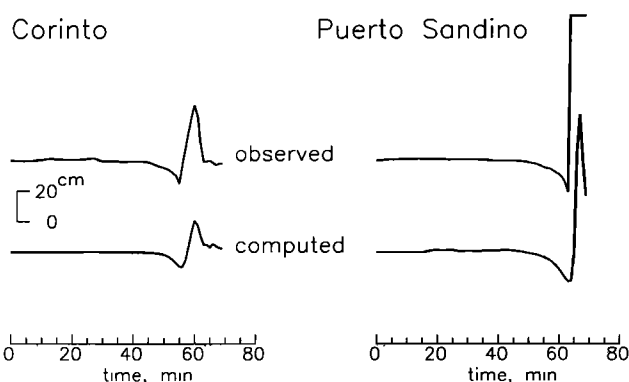


Figure 4. Comparison of the observed tsunami waveforms (top) and calculated (bottom) from the final source model using a non-linear tsunami computation.

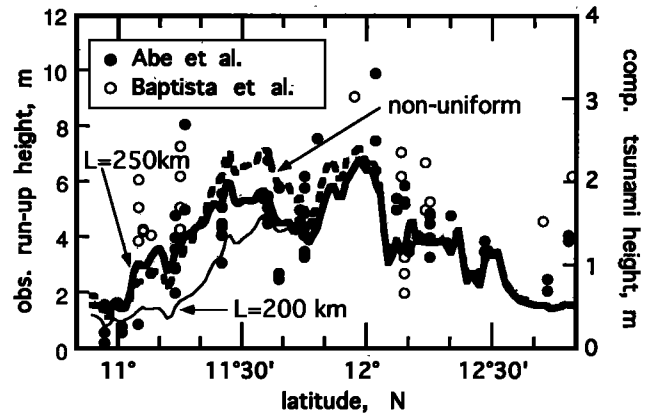


Figure 5. The observed tsunami run-up heights above MSL [*Abe et al.*, 1993; *Baptista et al.*, 1993] compared with the computed tsunami heights from the three different fault models: $L=200$ km, 250 km, and a heterogeneous slip distribution on $L=200$ km fault. Note the different vertical scales for the observed and computed tsunami heights.

dimensional linear computation with a one-dimensional non-linear run-up computation and successfully reproduced the tsunami run-up heights from a source model of *Imamura et al.* [1993]. The amplification factor thus may depend on the grid size of the computation.

Fault Length

A careful examination of Figure 5 shows that the observed pattern of run-up heights are larger along the southern coast of Nicaragua, namely between $11^{\circ}10'N$ and $50'$, than in the north. If the amplification factor is spatially constant, i.e., does not depend on the location, this suggests that slip distribution on the fault is different from what we modeled. In order to examine this, we modified the fault model in two different ways. One model is a longer ($L=250$ km) fault and the other has a larger (double) slip on the southern 50 km (the southernmost quarter of the 200 km long fault); this may represent an asperity. Both models have 1.25 times larger seismic moment than the previous model. Figure 5 also shows the computed tsunami heights from these models. The longer fault produces larger tsunami amplitudes between $10^{\circ}50'N$ and $11^{\circ}40'N$, while the non-uniform slip model produces larger tsunami amplitudes between $10^{\circ}50'N$ and $12^{\circ}N$. Comparison with the observed run-up height pattern shows that the longer fault with a uniform slip explains the observed pattern better. Hence we conclude that the fault length is 250 km, slightly longer than the seismological model.

Mechanism of Tsunami Earthquakes

The final fault parameters are: $L=250$ km, $W=40$ km, $u=3$ m. These are quite different than the seismological model of *Ide et al.* [1993] and we call it the tsunami model (Figure 6). As we have seen already, it extends only into the top 10 km of the crust. The rigidity around such a shallow fault may be smaller than the assumed value in the seismological model. If we use 1×10^{10} N/m² as the average rigidity for the top 10 km of crust, then the seismic moment becomes 3×10^{20} Nm for the tsunami model, which is in the range ($3-4 \times 10^{20}$ Nm) of values from the seismic wave analysis. In other words, both the seismic and tsunami models of the fault can explain the seismic observation, but only the tsunami model can explain the large tsunamis.

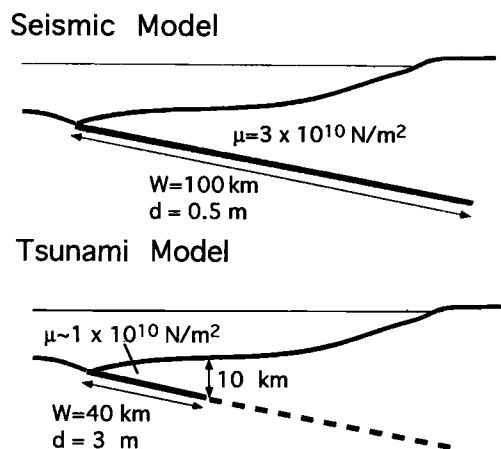


Figure 6. Schematic view of the seismic fault model (top) and the tsunami fault model (bottom). Both give the same seismic moment, but generate very different tsunamis.

Fukao [1979] explained the large tsunami excitation of the 1963 and 1975 Kuril tsunami earthquakes as a slip in the accretionary wedge. Okal [1988], based on normal mode theory, also showed that a tsunami source in the shallow sedimentary layer excites much larger tsunamis. The middle America trench off Nicaragua, however, does not have a large volume of sediments or a well-developed accretionary wedge [von Huene and Scholl, 1991; Kanamori and Kikuchi, 1993]. The sediments are completely subducted and the plate interface is filled with soft sediments. The rupture in such soft sediments would be slow and it explains the unusually long duration [Kanamori and Kikuchi, 1993]. The large tsunami excitation than expected from surface wave magnitude is partially due to the long duration. In addition, the shallow depth of the fault is also responsible to the large tsunamis. Hence the 1992 Nicaragua earthquake was a slow rupture on the shallow fault, presumably in the subducted sediments.

Acknowledgments. I thank Y. Fukao, H. Kanamori and Y. Tanioka for discussion, and J. Johnson for reading the manuscript. This work was supported by National Science Foundation (EAR-9117800).

References

Abe, K., K. Abe, Y. Tsuji, F. Imamura, H. Katao, Y. Iio, K. Satake, J. Bourgeois, E. Noguera, and F. Estrada, Field Survey of the Nicaragua

- earthquake and tsunami of September 2, 1992 (in Japanese), *Bull. Earthq. Res. Inst., Univ. of Tokyo*, 68, 23-70, 1993.
- Baptista, A.M., G.R. Priest, and T.S. Murty, Field survey of the 1992 Nicaragua tsunami, *Marine Geodesy*, 16, 169-203, 1993.
- Fukao, Y., Tsunami earthquakes and subduction processes near deep-sea trenches, *J. Geophys. Res.*, 84, 2303-2314, 1979.
- Ide, S., F. Imamura, Y. Yoshida, and K. Abe, Source characteristics of the Nicaragua tsunami earthquake of September 2, 1992, *Geophys. Res. Lett.*, 20, 863-866, 1993.
- Imamura, F., N. Shuto, S. Ide, Y. Yoshida, and K. Abe, Estimate of the tsunami source of the 1992 Nicaragua earthquake from tsunami data, *Geophys. Res. Lett.*, 20, 1515-1518, 1993.
- Kanamori, H., Mechanism of tsunami earthquakes, *Phys. Earth Planet. Inter.*, 6, 246-259, 1972.
- Kanamori, H., and M. Kikuchi, The 1992 Nicaragua earthquake: a slow tsunami earthquake associated with subducted sediments, *Nature*, 361, 714-716, 1993.
- Okada, Y., Surface deformation due to shear and tensile faults in a half-space, *Bull. Seism. Soc. Am.*, 75, 1135-1154, 1985.
- Okal, E.A., Seismic parameters controlling far-field tsunami amplitudes: a review, *Natural Hazards*, 1, 67-96, 1988.
- Pelayo, A.M., and D.A. Wiens, Tsunami earthquakes: slow thrust-faulting events in the accretionary wedge, *J. Geophys. Res.*, 97, 15321-15337, 1992.
- Satake, K., Linear and non-linear computations of the 1992 Nicaragua earthquake tsunamis, *Pure and Applied Geophysics*, in press, 1994.
- Satake, K., J. Bourgeois, K. Abe, K. Abe, Y. Tsuji, F. Imamura, Y. Iio, H. Katao, E. Noguera, and F. Estrada, Tsunami field survey of the 1992 Nicaragua earthquake, *Eos, Trans. Am. Geophys. Union*, 74, 145, 156-157, 1993.
- Shuto, N., Numerical simulation of tsunamis -its present and near future, *Natural Hazards*, 4, 171-191, 1991.
- Tadepalli, S., and C.E. Synolakis, The run-up of *N*-waves on sloping beaches, *Proc. R. Soc. London A*, 445, 99-112, 1994.
- Titov, V.V., and C.E. Synolakis, A numerical study of wave runup of the September 2, 1992 Nicaraguan tsunami, *Proc. IUGG/IIOC Int. Tsunami Symp.*, 627-635, 1993.
- von Huene, R. and D.W. Scholl, Observations at convergent margins concerning sediment subduction, subduction erosion, and the growth of continental crust, *Rev. Geophys.*, 29, 279-316, 1991.

K. Satake, Dept. of Geological Sciences, Univ. of Michigan, Ann Arbor, MI 48109-1063. (e-mail: kenji@umich.edu)

(Received: June 3, 1994; revised August 5, 1994; accepted August 11, 1994.)